Biochemical Pharmacology, Vol. 38, No. 5, pp. 837–850, 1989.
Printed in Great Britain.

0006-2952/89 $3.00 + 0.00

AUTORADIOGRAPHIC ANALYSES OF AGONIST BINDING TO MUSCARINIC RECEPTOR SUBTYPES*

WILLIAM S. MESSER, JR.,† BRENDA ELLERBROCK, MAUREEN PRICE‡ and WAYNE HOSS
Department of Medicinal Chemistry, College of Pharmacy, University of Toledo, Toledo, OH 43606, U.S.A.

(*Received* 25 *April* 1988; *accepted* 3 *August* 1988)

Abstract—The binding of four muscarinic receptor agonists to regions of rat brain was examined through quantitative autoradiographic techniques. Oxotremorine, arecoline, pilocarpine and bethanechol were chosen based on their different potencies and efficacies in muscarinic second messenger systems. Overall, the order of potency for inhibition of [^{3}H]-*l*-quinuclidinyl benzilate ([^{3}H]-*l*-QNB) binding to rat brain slices was oxotremorine > pilocarpine = arecoline ≫ bethanecol. Regional assays of agonist potency indicated that all agonists were more selective for brainstem and thalamic regions than for hippocampal and cortical regions. The high selectivity of agonists for areas such as the paraventricular thalamus and the superior colliculus, which also display low affinity for pirenzepine, suggests that muscarinic agonists bind with higher affinity to M_2 receptors. Of the four agonists examined, pilocarpine displayed the lowest selectivity for M_2 receptors in that IC_{50} values for pilocarpine were only 3-fold higher in the hippocampal and striatal regions (e.g. CA3: 40.6 ± 9.4 μM) than in thalamic and brainstem regions (e.g. paraventricular thalamus: 14.9 ± 6.2 μM). Oxotremorine was 8-fold more potent in the brainstem and thalamus, while arecoline and bethanechol were, respectively, 19- and 100-fold more selective for brainstem and thalamic receptors. Scatchard analyses revealed heterogeneous binding profiles for some agonists within single brain regions, suggesting that multiple agonist sites exist even within regions of predominately M_1 or M_2 receptors. For example, arecoline displayed curved Scatchard plots within the external layers of the cerebral cortex, layer CA1 of the hippocampus (predominantly M_1 subtype), and the paraventricular thalamus (predominantly M_2 subtype). The ability of agonists to recognize multiple sites within a single region may reflect the ability to recognize receptors coupled or uncoupled to second messenger systems through G-proteins.

Muscarinic receptor agonists display heterogeneous binding profiles in brain membrane preparations [1, 2]. Full agonists such as carbamylcholine distinguish among at least three subclasses of muscarinic sites based on agonist affinity. Autoradiographic studies on brain sections have revealed similar binding profiles including regional variations in sites of higher affinity [3–5]. The pattern of muscarinic binding indicates that muscarinic receptors in the brainstem nuclei (e.g. superior colliculus) possess a higher affinity for carbamylcholine than receptors in the forebrain (e.g. cortex, dentate gyrus).

The binding of selective antagonists to muscarinic receptors has led to the proposed subclasses of M_1 and M_2 muscarinic receptors [6]. In binding assays using brain homogenates, pirenzepine displays a selectivity for M_1 receptors found predominantly in the forebrain [7], whereas gallamine and AF-DX 116 bind selectively to muscarinic receptors in the brainstem and heart [8–11]. In brain, the distribution of high-affinity gallamine sites and high-affinity carbamylcholine sites is similar, while high-affinity pirenzepine sites appear to correspond to low-affinity carbamylcholine sites [3–5, 12–14].

Muscarinic receptors in brain are linked to the inhibition of adenylate cyclase, stimulation of phosphoinositide turnover, and modulation of acetylcholine release. Muscarinic agonists differ in their abilities to activate these systems. Oxotremorine and arecoline are potent inhibitors of adenylate cyclase activity in rat striatum [15]. In contrast, both oxotremorine and arecoline as well as pilocarpine are poor stimulators of labeled inositol phosphate release in guinea pig cerebral cortex and hippocampus [16]. Bethanechol is less potent and efficacious than oxotremorine or arecoline in the inhibition of adenylate cyclase in rat striatum [15], yet is more efficacious than pilocarpine, arecoline and oxotremorine in stimulating phospholipid (phosphatidyl inositol and phosphatidate) labeling in rat and guinea pig nerve endings prepared from the cerebral cortex [17].

Studies on the binding of agonists to muscarinic receptor subtypes have demonstrated the selectivity of pilocarpine for M_1 receptors, indicated by a lack of guanine nucleotide sensitivity in pilocarpine binding to rat cortical membranes labeled with either [^{3}H]QNB‖ or [^{3}H]pirenzepine in modified Krebs-phosphate buffer [18]. Oxotremorine is relatively

* This work was supported in part by Research Grant NS 23929 and a Research Challenge Grant from the Ohio Board of Regents.

† Correspondence: William S. Messer, Jr., Ph.D., Department of Medicinal Chemistry, College of Pharmacy, University of Toledo, 2801 West Bancroft St., Toledo, OH 43606.

‡ Present address: Department of Neurology, 1009 Howard Bldg., Memorial Sloan-Kettering Cancer Center, 1275 York Ave., New York, NY 10028.

‖ Abbreviations: QNB, quinuclidinyl benzilate; and CA, cornu ammonis of the hippocampus.

nonselective for muscarinic receptor subtypes under the same conditions (i.e. guanine nucleotides modulate oxotremorine binding to sites labeled by either [^{3}H]QNB or [^{3}H]pirenzepine). Furthermore, oxotremorine is able to inhibit the release of acetylcholine in striatal slices [19], although pilocarpine is much weaker than oxotremorine in similar preparations [20, 21].

The relationship between the binding profiles for the agonists and their abilities to stimulate or inhibit one or more second messenger systems is unknown. Although the binding of partial muscarinic agonists has been studied previously [4], a systematic examination of partial agonists with different potencies and efficacies for second messenger systems is needed. To better understand the relationship between selective agonists and second messenger systems as well as the relative selectivity of partial agonists for muscarinic receptor subtypes, we have examined the binding properties of four muscarinic agonists both in whole sections and after autoradiographic localization of muscarinic receptor binding sites. The autoradiographic method was chosen because it has a higher resolution compared with conventional membrane binding assays and also because of the large number of discrete regions that can be sampled in a single assay. Although the agonists have disparate abilities to activate second messenger systems, they all appear to be M_2-selective.

METHODS

Materials. [^{3}H]-*l*-Quinuclidinyl benzilate ([^{3}H]-*l*-QNB) was purchased from Amersham with a specific activity of 30 Ci/mmol. Tritium standards ([^{3}H]Microscales) (3–100 nCi/mg) were also purchased from Amersham. Pilocarpine, arecoline, oxotremorine, and bethanechol were purchased from Sigma. [^{3}H]-Sensitive Ultrofilm was purchased from LKB Industries.

Binding assays. The methods for measuring inhibition of [^{3}H]-*l*-QNB binding to rat brain slices were adapted from previous studies [3, 5, 13, 22]. Briefly, in the experiments presented here, rats were killed by cardiac perfusion with 50 ml of 40 mM sodium, potassium phosphate buffer, pH 7.4, followed by 0.1% formaldehyde in buffer (200 ml). Each brain was rapidly removed, frozen over liquid nitrogen, and stored at −20° until sectioned using a cryostat. Twelve micron-thick coronal sections were taken serially and mounted on acid-washed slides coated with chromium potassium sulfate and gelatin. Slides were stored in microscope slide boxes at −20° until used in the binding assay.

Slides were incubated in Coplin jars with 40 mM sodium, potassium phosphate buffer, pH 7.4, and several concentrations of [^{3}H]-*l*-QNB (0.2 to 2 nM) for 2 hr. One jar at each concentration included an excess (1000-fold) of unlabeled atropine to measure nonspecific binding. For the indirect binding assays, slides were incubated with 0.2 nM [^{3}H]-*l*-QNB in the presence of increasing concentrations of unlabeled ligands for 2 hr. Equilibrium is attained for both direct and indirect binding assays within 2 hr. Following the incubation period, sections were rinsed in buffer twice for 10 min. One section from each slide was wiped onto a filter paper and placed in a Nalge bag for standard scintillation counting. The final concentration of [^{3}H]-*l*-QNB was measured by removing aliquots from each jar for counting. The slides were dried and placed back in slide boxes and stored at −20° until they were apposed to film. Data analysis included determination of the B_{max} and the apparent dissociation constant [K_d(app)] from Scatchard plots for [^{3}H]-*l*-QNB binding. Inhibition values were determined for each competing ligand. The data were analyzed to generate Hill and Eadie–Hofstee plots.

Film processing and image analysis. Slides were apposed to LKB tritium-sensitive Ultrofilm in the dark by placing the slides in film cassettes, pressing the film firmly against the slides, closing the cassette, and wrapping it in a dark cloth for 7–9 days. At the end of the exposure period, the film was developed using Kodak D-19 developer for 5 min, rinsed in a stop bath for 30 sec, and fixed with Kodak rapid fixer for another 5 min. After a 20-min rinse in water, the film was dipped into a Photo-flo solution for 30 sec and air-dried.

Images were analyzed using the RAS1000 system developed by Loats Associates for the Amersham Corp. Tritium standards ([^{3}H]Microscales) (3–100 nCi/mg) were used for quantifying the autoradiograms. Density readings for standards of known radioactivity were taken for comparison of optical density to isotope levels on each sheet of film. Standard curves for converting optical density to disintegrations per minute values were best fit by linear transformation. Background readings of optical density and levels of nonspecific binding were used in determining the relative amount of drug specifically bound to each section for the indirect assays. Several regions of each image were examined for labeling by [^{3}H]-*l*-QNB. Regions were identified using an atlas of the rat brain [23]. The amount of [^{3}H]-*l*-QNB bound to each area was expressed as the mean for each slide (three sections per slide). Data taken from areas found in both the left and right hemispheres were pooled from each section to determine the overall mean for that region of brain.

The IC_{50} values and Hill slopes were calculated for each region of brain from Hill plots generated from the data on each individual animal. The IC_{50} values and Hill slopes were then combined to give a mean (± SEM) for each brain region and each agonist.

RESULTS

Binding to rat brain sections. Overall binding parameters were derived from data obtained with whole slices and represent means of all rostral-caudal levels sampled. The binding of [^{3}H]-*l*-QNB to rat brain slices was similar to that described previously [3, 5, 13, 24]. Analysis of the binding curves indicated a K_d(app) of 0.5 nM with a B_{max} of 0.3 pmol/slice [5].

Oxotremorine was the most potent inhibitor of [^{3}H]-*l*-QNB binding to rat brain slices, while arecoline and pilocarpine displayed an intermediate potency and bethanechol possessed the lowest potency (Table 1). Analysis of binding parameters (e.g. Hill slopes) to rat brain slices suggested that

Table 1. Binding of oxotremorine, arecoline, bethanechol and pilocarpine to rat brain slices

Ligand	Hill slope	IC_{50} (μM)
Oxotremorine	0.91 ± 0.05	4.1 ± 0.8
Pilocarpine	1.11 ± 0.12	19.9 ± 4.0
Arecoline	0.67 ± 0.05	24.5 ± 5.9
Bethanechol	0.82 ± 0.03	504 ± 42

Data were generated from Hill plots using pooled means (± SEM) from at least three animals for binding to whole slices.

bethanechol, arecoline, and perhaps oxotremorine distinguished between classes of receptors, whereas pilocarpine appeared to label only a single population of muscarinic receptors.

Regional binding of muscarinic agonists. Inhibition curves (Figs. 1–4) for agonist binding to rat brain sections were generated from autoradiograms as found in Figs. 5–8. Data generated from autoradiograms were analyzed to determine the levels of inhibition for each ligand within selected brain regions. From the raw data for each animal, the IC_{50} values and Hill slopes were calculated for each brain region. The values were then used to determine the overall means for the group of animals used in the experiments.

The Hill slopes and IC_{50} values for oxotremorine, bethanechol, arecoline and pilocarpine are shown in Table 2. Oxotremorine displayed the highest potency

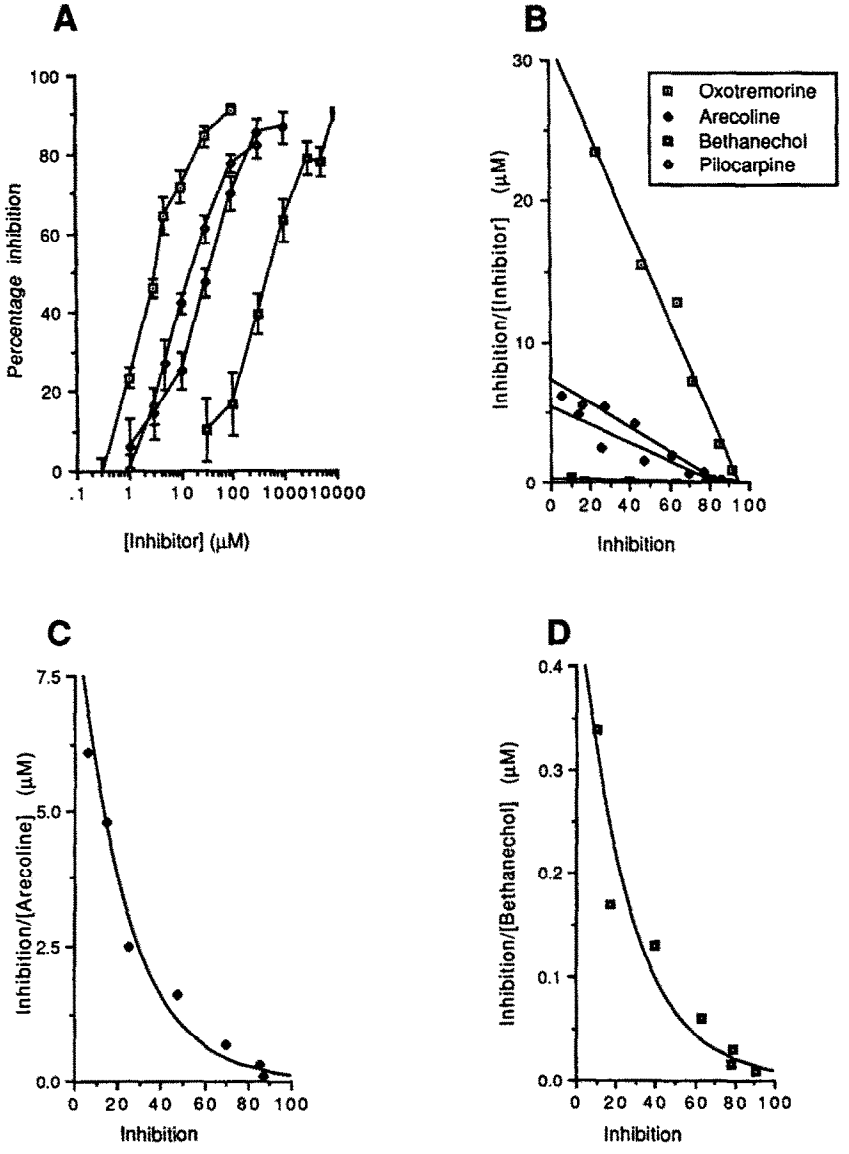

Fig. 1. Inhibition of [^{3}H]-*l*-QNB binding by muscarinic agonists in the cerebral cortex. (A) Log dose–response curves for oxotremorine, arecoline, bethanechol and pilocarpine. Values are means ± SEM, N = 3. (B) Scatchard-type plot of the same data. (C) Expanded plot of arecoline binding to the cerebral cortex. (D) Expanded plot of bethanechol binding to the cerebral cortex. Units on the abscissa of panels B–D: percent inhibition.

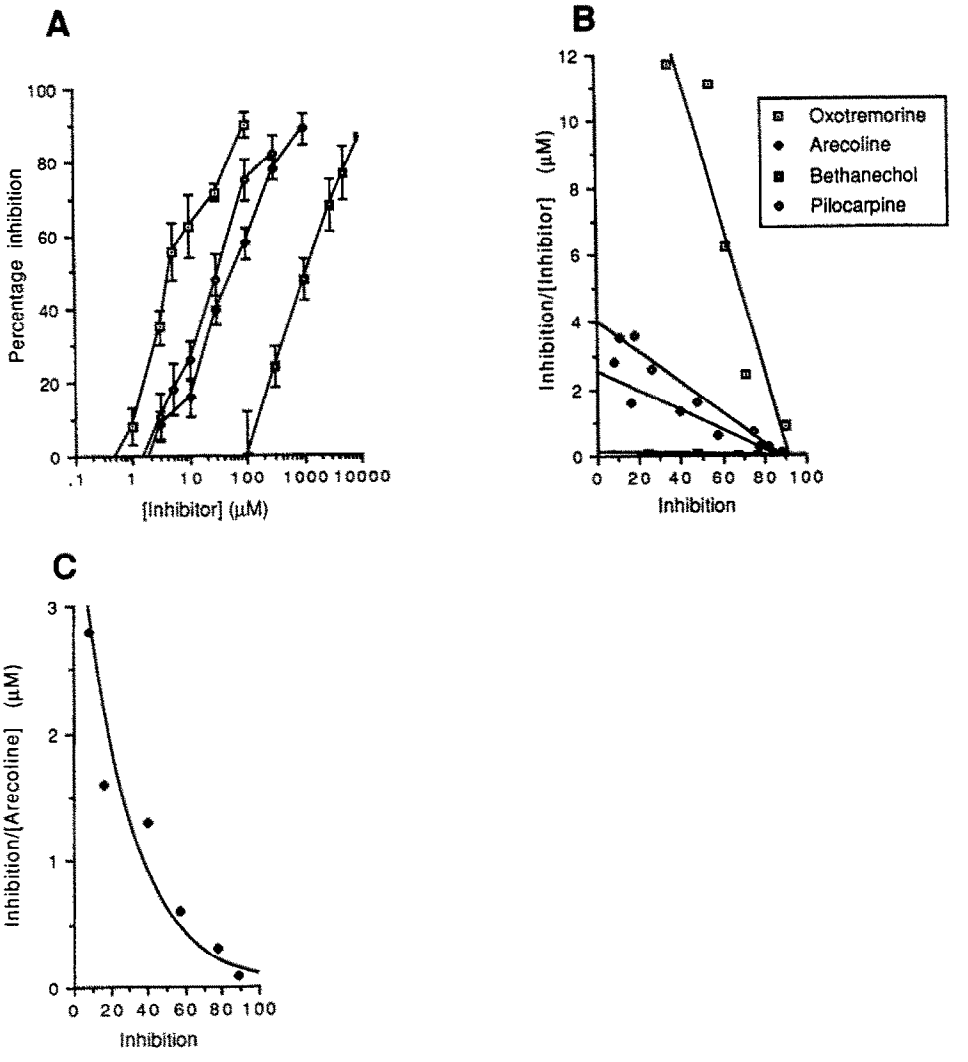

Fig. 2. Inhibition of [^{3}H]-*l*-QNB binding by muscarinic agonists in the CA1 region of the hippocampus. (A). Log dose–response curves for oxotremorine, arecoline, bethanechol and pilocarpine. Values are means ± SEM, N = 3. (B) Scatchard-type plot of the same data. (C) Expanded plot of arecoline binding to the CA1 region of the hippocampus. Units on the abscissa of panels B and C: percent inhibition.

of all agonists with IC_{50} values ranging from 11.6 μM in the striatum to 0.98 μM in the paraventricular thalamus. In contrast, bethanechol displayed the lowest affinity for muscarinic receptors with IC_{50} values ranging from 1.4 mM in the dentate gyrus to 12.9 μM in the paraventricular thalamus.

Within a single brain region such as the cerebral cortex (see Fig. 1, A and B), the rank-order of potency was oxotremorine > pilocarpine ≥ arecoline ≥ bethanechol. The same relationship held within the CA1 region of the hippocampus (Fig. 2, A and B), although Hill slopes within the cerebral cortex were generally less than unity while near unity for the CA1 and dentate gyrus (see Table 2). Muscarinic agonists displayed no dissimilarity in binding when comparing the different layers of the cerebral cortex. Bethanechol was more potent in binding to the cingulate cortex than to other cortical layers, whereas oxotremorine, pilocarpine and arecoline did not possess a higher affinity for the cingulate cortex (see Table 2).

Eadie–Hofstee analyses of the binding of agonists revealed some interesting differences between ligands within the cerebral cortex (see Fig. 1B). The binding of oxotremorine and pilocarpine fit a single-site model as can be seen by the linearity of the plotted data. The binding curves for arecoline and bethanechol were not linear, suggesting the possibility for multiple sites within the cerebral cortex (see Fig. 1, C and D).

Arecoline binding to sites within the hippocampus also displayed a nonlinear Scatchard profile (see Fig. 2C), while the binding of oxotremorine, pilocarpine and bethanechol fit a single-site model (Fig. 2B). Within the caudate nucleus, bethanechol was the only agonist for which multiple sites could be distin-

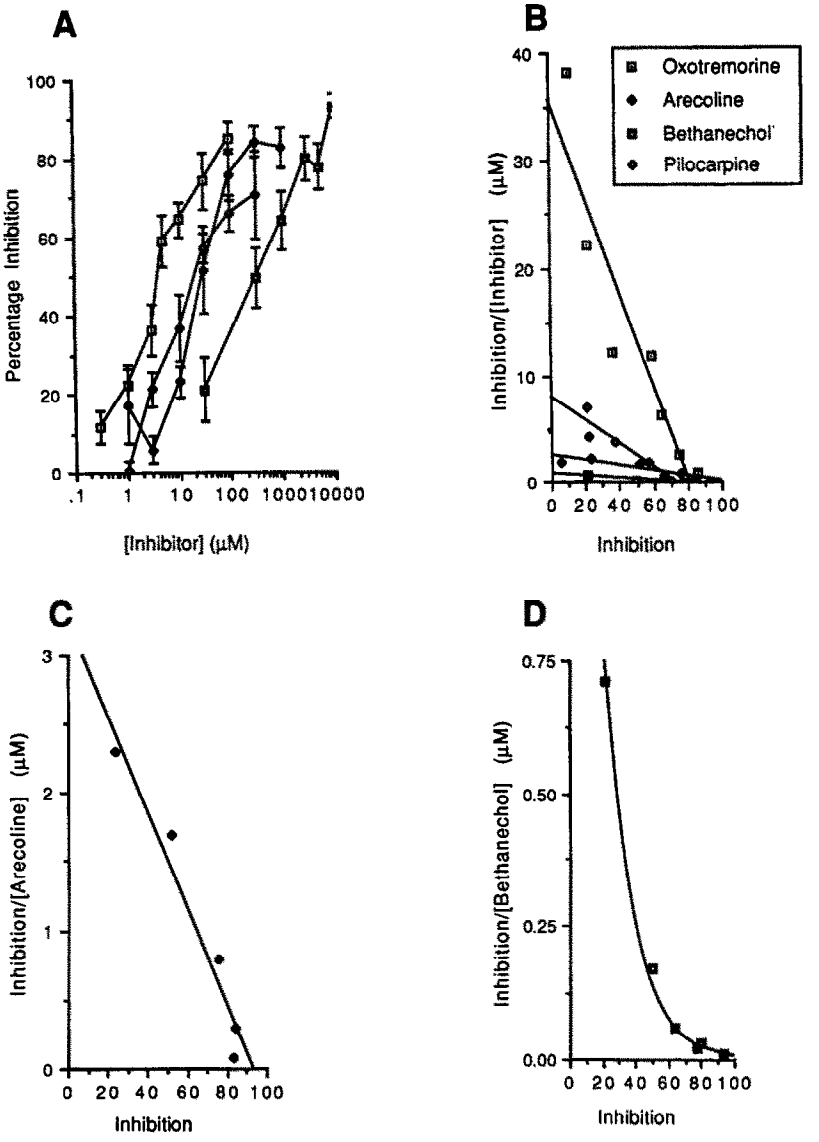

Fig. 3. Inhibition of [^{3}H]-*l*-QNB binding by muscarinic agonists in the caudate nucleus. (A) Log dose–response curves for oxotremorine, arecoline, bethanechol and pilocarpine. Values are means ± SEM, N = 3. (B) Scatchard-type plot of the same data. (C) Expanded plot of arecoline binding to the caudate nucleus. (D) Expanded plot of bethanechol binding to the caudate nucleus. Units on the abscissa of panels B–D: percent inhibition.

guished from Scatchard analyses (see Fig. 3, B and D). Pilocarpine binding fit a single-site model, but only 72.6% of the sites labeled by [^{3}H]-*l*-QNB were inhibited (Fig. 3B).

A consistent profile of agonist selectivity in the forebrain was reflected in the amygdaloid nuclei when comparing inhibition values for each muscarinic agonist. The order of potency was oxotremorine > arecoline = pilocarpine ⩾ bethanechol for the medial and central amygdaloid nuclei. The same relationship held for the basolateral and lateral nuclei although the potency was approximately three times lower in both the basolateral and lateral nuclei for each ligand than in the central and medial nuclei (see Table 2).

In contrast to the forebrain regions, midbrain areas displayed a different profile of agonist binding, as shown in Table 2. For example, within the medial dorsal nucleus of the thalamus, the rank-order of potency was oxotremorine > arecoline > pilocarpine ⩾ bethanechol. Within the paraventricular nucleus of the thalamus, the rank-order of potency was oxotremorine > arecoline > bethanechol ⩾ pilocarpine. The differences observed may be considered to reflect the relatively high selectivity (when compared to other agonists) of pilocarpine for forebrain as opposed to midbrain and brainstem receptors. For example, the potency of pilocarpine for the paraventricular thalamic nucleus (14.9 ± 6.2 μM) was within the range of binding for

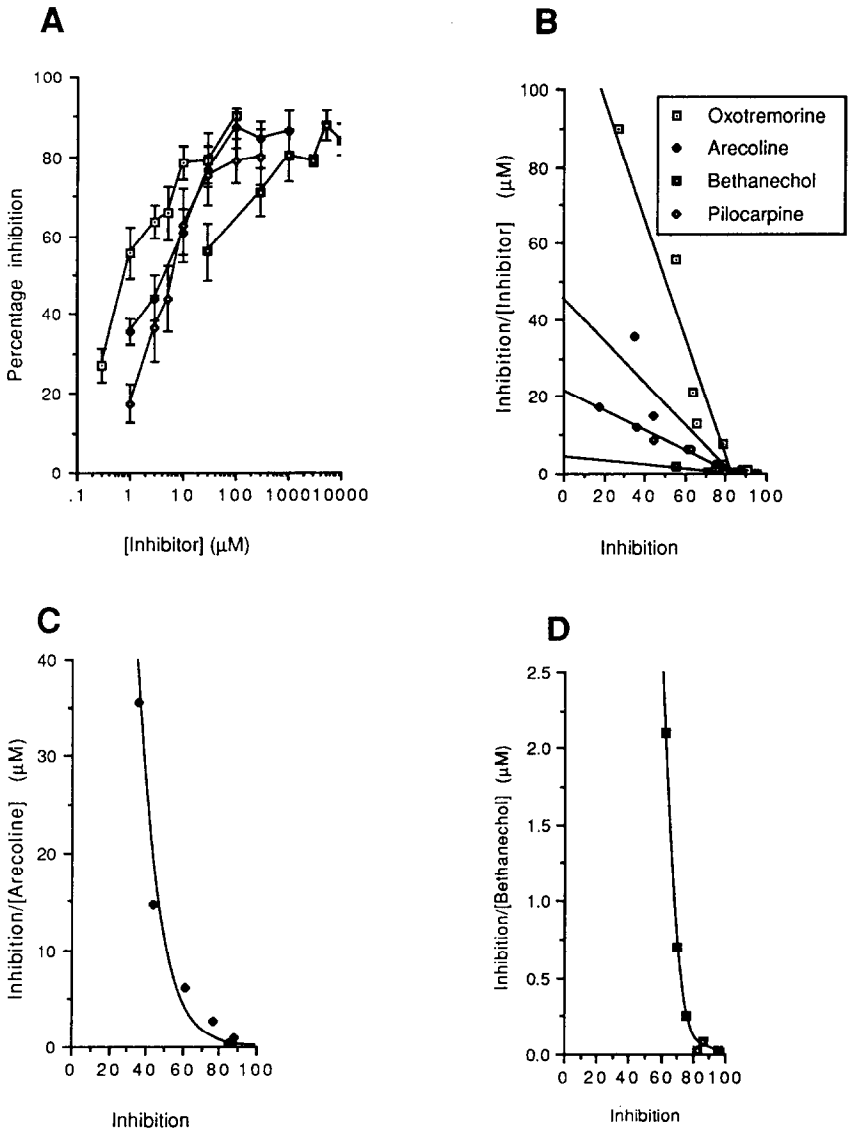

Fig. 4. Inhibition of [^{3}H]-*l*-QNB binding by muscarinic agonists in the paraventricular thalamus. (A) Log dose–response curves for oxotremorine, arecoline, bethanechol and pilocarpine. Values are means ± SEM, N = 3. (B) Scatchard-type plot of the same data. (C) Expanded plot of arecoline binding to the paraventricular thalamus. (D) Expanded plot of bethanechol binding to the paraventricular thalamus. Units on the abscissa of panels B–D: percent inhibition.

the cerebral cortex (23.5 ± 4.6 μM). In contrast, bethanechol was nearly two orders of magnitude more potent in the paraventricular thalamus than in the cerebral cortex (see Table 2). Furthermore, pilocarpine was slightly more potent than arecoline in all forebrain areas, yet was less potent than arecoline in all thalamic regions. The differences between pilocarpine and arecoline are most evident from Scatchard-type analyses. In the cerebral cortex (Fig. 1, B, C and D) and paraventricular thalamus (Fig. 4, B, C and D), both oxotremorine and pilocarpine labeled a single site, whereas in the same regions bethanechol and arecoline appeared to distinguish at least two sites.

DISCUSSION

The major finding of the present study was that the binding of selective muscarinic agonists followed more closely the pattern of binding found for the selective muscarinic antagonist gallamine [13] than that found for pirenzepine [5]. Pirenzepine binds to M_1 receptors in the rat forebrain [7], whereas gallamine binds with higher affinity to M_2 sites [10, 13]. Overall, the binding of oxotremorine, arecoline, pilocarpine and bethanechol was remarkably similar to carbamylcholine with regard to regional selectivity [5]. In general, high-affinity agonist sites are found in brainstem and thalamic regions, while

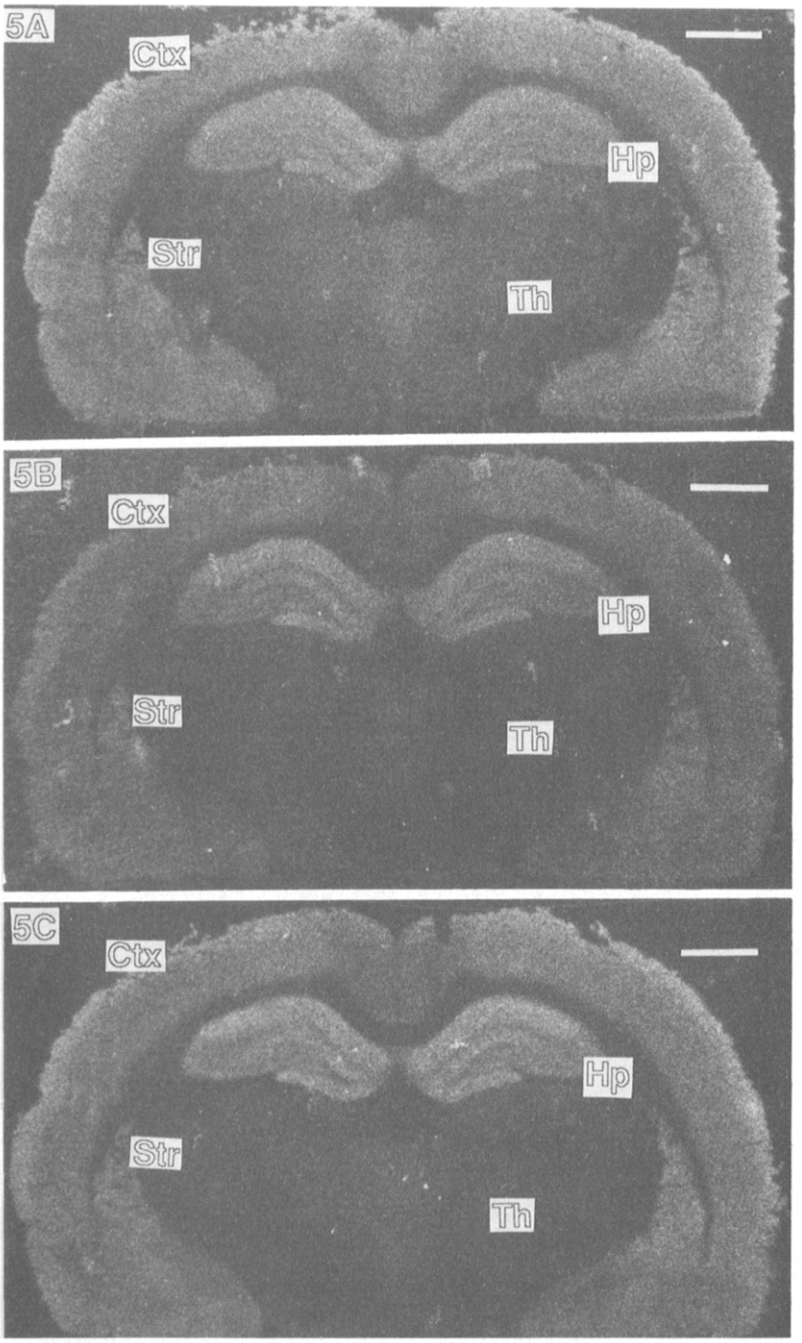

Fig. 5. Binding of arecoline and bethanechol to muscarinic receptors at the level of the dorsal hippocampus (Hp) in rat brain. (A) Binding of [^{3}H]-*l*-QNB to muscarinic receptors. Regions depicted in these sections include the cerebral cortex (Ctx), striatum (Str) and various thalamic nuclei (Th). 1 cm = 1.5 mm. (B) Inhibition of [^{3}H]-*l*-QNB binding by 30 μM arecoline. Note the nearly complete inhibition in the thalamus while hippocampal regions remained labeled. (C) Inhibition of [^{3}H]-*l*-QNB binding by 100 μM bethanechol. The relatively low affinity of bethanechol is indicated by the lower level of inhibition despite the higher concentration.

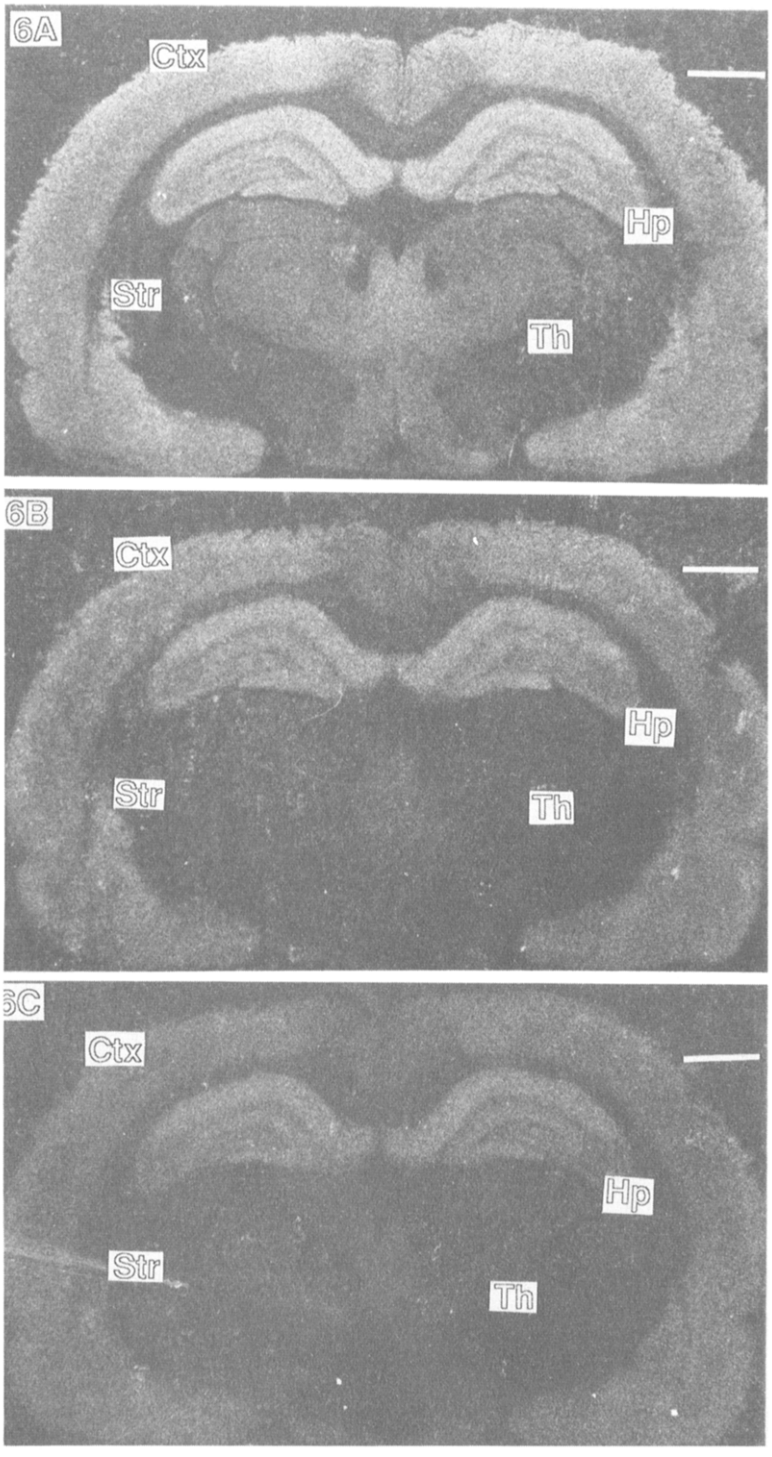

Fig. 6. Binding of pilocarpine and oxotremorine to muscarinic receptors at the level of the dorsal hippocampus (Hp) in rat brain. (A) Binding of [^{3}H]-*l*-QNB to muscarinic receptors. Regions depicted in these sections include the cerebral cortex (Ctx), striatum (Str) and various thalamic nuclei (Th). 1 cm = 1.5 mm. (B) Inhibition of [^{3}H]-*l*-QNB binding by 5 μM pilocarpine. Note the nearly complete inhibition in the thalamus while hippocampal regions remained labeled. (C) Inhibition of [^{3}H]-*l*-QNB binding by 3 μM oxotremorine. The relatively high affinity of oxotremorine can be seen in nearly every brain region.

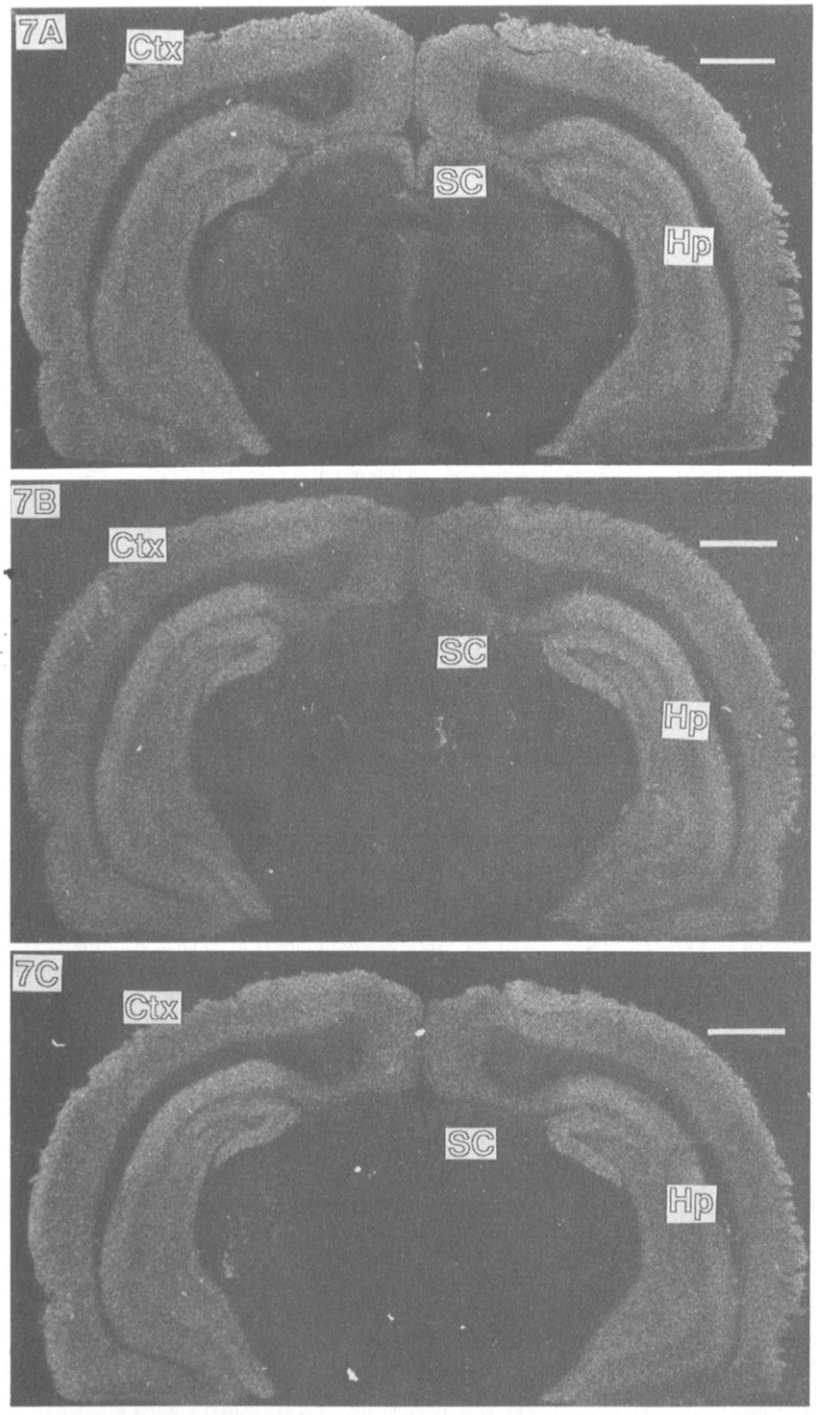

Fig. 7. Binding of arecoline and bethanechol to muscarinic receptors at the level of the superior colliculus (SC) in rat brain. (A) Binding of [^{3}H]-*l*-QNB to muscarinic receptors. Other regions depicted in these sections include the cerebral cortex (Ctx), and the hippocampus (Hp). 1 cm = 1.5 mm. (B) Inhibition of [^{3}H]-*l*-QNB binding by 30 μM arecoline. Note the nearly complete inhibition in the brainstem while hippocampal regions remained labeled. (C) Inhibition of [^{3}H]-*l*-QNB binding by 100 μM bethanechol.

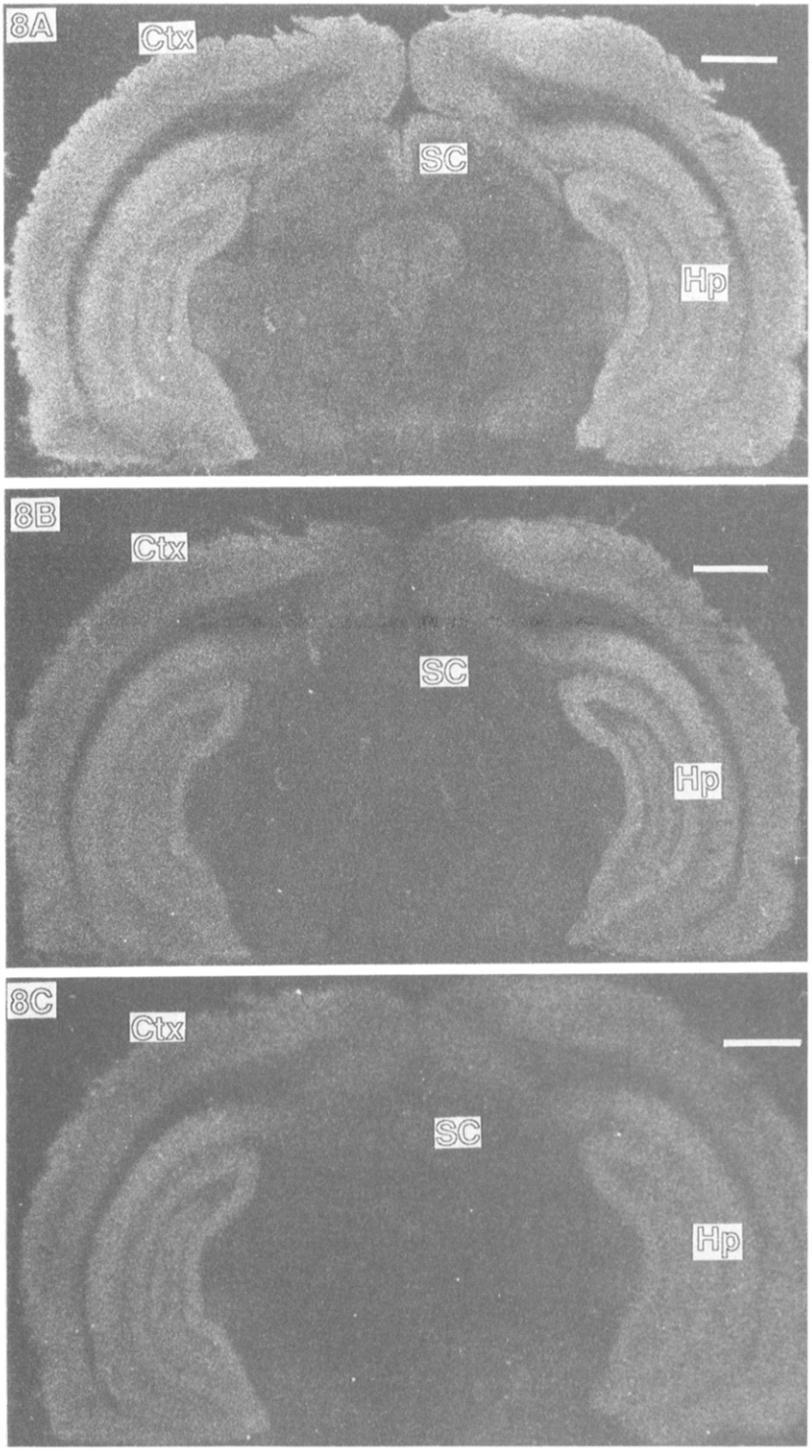

Fig. 8. Binding of pilocarpine and oxotremorine to muscarinic receptors at the level of the superior colliculus (SC) in rat brain. (A) Binding of [^{3}H]-*l*-QNB to muscarinic receptors. Other regions depicted in these sections include the cerebral cortex (Ctx), and the hippocampus (Hp). 1 cm = 1.5 mm. (B) Inhibition of [^{3}H]-*l*-QNB binding by 10 μM pilocarpine. (C) Inhibition of [^{3}H]-*l*-QNB binding by 3 μM oxotremorine.

Table 2. Binding of oxotremorine, arecoline, bethanechol and pilocarpine to various regions of rat brain

Brain region	Bethanechol		Arecoline		Pilocarpine		Oxotremorine	
	Hill slope	IC_{50} (μM)	Hill slope	IC_{50} (μM)	Hill slope	IC_{50} (μM)	Hill slope	IC_{50} (μM)
Cerebral cortex (layers 1–3)	0.711 ± 0.068	810 ± 248	0.675 ± 0.041	36.8 ± 3.0	0.835 ± 0.062	23.5 ± 4.6	0.729 ± 0.029	3.78 ± 0.63
Cerebral cortex (layers 4–5)	0.714 ± 0.086	604 ± 17	0.578 ± 0.036	41.9 ± 6.2	0.713 ± 0.054	27.9 ± 6.8	0.816 ± 0.054	5.79 ± 1.30
Cerebral cortex (layer 6)	0.649 ± 0.058	764 ± 74	0.559 ± 0.054	48.1 ± 7.5	0.761 ± 0.091	32.9 ± 9.1	0.820 ± 0.077	6.27 ± 1.50
Cingulate cortex	0.652 ± 0.092	212 ± 19	0.661 ± 0.092	31.4 ± 12.1	0.685 ± 0.065	19.9 ± 3.8	0.678 ± 0.018	3.84 ± 1.12
Entorhinal cortex	0.774 ± 0.080	1341 ± 84.2	0.687 ± 0.099	86.1 ± 24.7	—	—	—	—
Primary olfactory cortex	0.865 ± 0.096	1320 ± 460	0.666 ± 0.097	97.4 ± 11.15	—	—	—	—
CA1	0.918 ± 0.209	1120 ± 100	0.857 ± 0.150	58.4 ± 6.3	0.890 ± 0.015	35.4 ± 12.2	1.085 ± 0.118	10.9 ± 3.97
CA3	0.906 ± 0.008	600 ± 51	0.818 ± 0.127	50.1 ± 10.8	0.939 ± 0.084	40.6 ± 9.4	0.742 ± 0.016	6.17 ± 1.39
Dentate gyrus	1.372 ± 0.268	1430 ± 258	1.008 ± 0.153	66.5 ± 6.8	0.935 ± 0.046	43.3 ± 10.6	0.988 ± 0.065	8.17 ± 1.83
Lateral amygdala	1.046 ± 0.186	716 ± 217	0.940 ± 0.139	58.3 ± 5.3	0.683 ± 0.012	44.3 ± 18.9	0.828 ± 0.047	7.24 ± 2.05
Central amygdala	0.667 ± 0.096	479 ± 212	0.788 ± 0.123	37.6 ± 4.2	0.626 ± 0.098	23.4 ± 5.5	0.730 ± 0.055	4.47 ± 0.90
Basolateral amygdala	0.713 ± 0.291	593 ± 462	0.764 ± 0.042	50.4 ± 8.4	0.785 ± 0.060	55.7 ± 11.5	0.991 ± 0.074	8.66 ± 0.95
Medial amygdala	0.675 ± 0.829	220 ± 68.7	0.709 ± 0.078	16.5 ± 3.3	0.694 ± 0.150	14.4 ± 5.1	0.560 ± 0.015	2.84 ± 0.53
Posteromedial cortical amygdala	—	—	—	—	0.856 ± 0.081	16.6 ± 6.3	—	1.48 ± 1.16
Ventrolateral caudate putamen	0.887 ± 0.175	1195 ± 569	0.760 ± 0.116	109 ± 27.0	0.832 ± 0.015	57.4 ± 9.6	0.934 ± 0.143	11.6 ± 2.91
Dorsomedial caudate putamen	0.454 ± 0.129	438 ± 181	0.756 ± 0.187	40.5 ± 10.6	0.678 ± 0.087	39.6 ± 8.5	0.670 ± 0.064	5.66 ± 0.48
Olfactory tubercle	0.186 ± 0.038	356 ± 243	0.412 ± 0.128	49.5 ± 18.5	0.485 ± 0.024	35.5 ± 16.7	—	—
Stria terminals, bed nucleus	0.507 ± 0.159	390 ± 109	0.489 ± 0.204	51.7 ± 34.2	0.524 ± 0.177	15.6 ± 5.7	0.429 ± 0.133	3.63 ± 3.07
Lateral septal nucleus	0.258 ± 0.013	91.0 ± 46.6	0.266 ± 0.049	36.5 ± 27.4	0.528 ± 0.039	10.7 ± 4.3	0.458 ± 0.053	2.70 ± 1.69
Posterior hypothalamus	0.295 ± 0.006	140 ± 73.6	0.277 ± 0.080	49.4 ± 59.4	0.469 ± 0.013	9.06 ± 4.81	0.337 ± 0.030	1.26 ± 0.87
Anterior hypothalamus	0.563 ± 0.255	115 ± 88.0	0.715 ± 0.406	27.2 ± 25.6	0.641 ± 0.267	14.8 ± 6.1	—	2.00 ± 0.07
Medial dorsal thalamus	0.597 ± 0.089	78.2 ± 20.8	0.736 ± 0.092	6.8 ± 2.5	0.580 ± 0.027	23.6 ± 11.7	0.416 ± 0.045	2.68 ± 1.62
Central medial thalamus	0.519 ± 0.068	58.1 ± 14.4	0.568 ± 0.056	6.3 ± 1.0	0.856 ± 0.243	10.2 ± 4.3	0.575 ± 0.071	2.86 ± 1.01
Lateral posterior thalamus	0.370 ± 0.019	155 ± 12.4	0.318 ± 0.027	11.2 ± 0.4	0.521 ± 0.037	28.5 ± 14.2	0.390 ± 0.072	2.90 ± 1.46
Paraventricular thalamus	0.355 ± 0.098	12.9 ± 7.1	0.421 ± 0.064	3.5 ± 0.7	0.509 ± 0.015	14.9 ± 6.2	0.431 ± 0.008	0.98 ± 0.48
Dorsal lateral geniculate	0.337 ± 0.039	176 ± 10.0	0.542 ± 0.275	15.3 ± 8.9	0.475 ± 0.044	19.1 ± 9.5	0.466 ± 0.045	3.59 ± 2.16
Reticular thalamus	0.406 ± 0.209	91.7 ± 54.6	0.243 ± 0.058	6.6 ± 2.6	0.300 ± 0.046	—	0.260 ± 0.039	7.22 ± 4.77
Lateral dorsal thalamus	0.399 ± 0.272	47.8 ± 31.4	—	5.8 ± 1.2	0.942 ± 0.137	23.6 ± 12.3	0.517 ± 0.064	3.37 ± 1.94
Rhomboid thalamus	0.634 ± 0.085	76.4 ± 27.5	0.581 ± 0.039	6.0 ± 0.8	0.839 ± 0.161	18.4 ± 8.2	0.581 ± 0.040	2.11 ± 0.53
Reuniens thalamus	0.605 ± 0.133	65.1 ± 0.4	0.398 ± 0.041	5.0 ± 1.5	0.661 ± 0.037	15.0 ± 9.4	0.549 ± 0.011	2.22 ± 0.59
Posterior thalamus	0.359 ± 0.037	173 ± 131	0.402 ± 0.092	20.9 ± 15.3	0.577 ± 0.019	51.4 ± 25.4	0.464 ± 0.045	4.31 ± 1.87
Substantia nigra	0.600 ± 0.034	341 ± 90.1	0.448 ± 0.070	144 ± 106	—	—	—	—
Interpeduncular nucleus	0.518 ± 0.157	90.0 ± 33.1	0.351 ± 0.095	44.4 ± 40.7	—	—	—	—
Superior colliculus	0.454 ± 0.129	25.7 ± 13.6	0.425 ± 0.090	1.5 ± 0.3	0.800 ± 0.172	7.11 ± 4.21	—	—
Periaquaeductal gray	0.375 ± 0.106	16.3 ± 6.4	0.308 ± 0.086	1.4 ± 0.3	—	—	—	—
Trigeminal nucleus	0.697 ± 0.386	35.1 ± 23.1	0.291 ± 0.082	2.6 ± 1.8	—	—	—	—
Cerebellum	—	—	0.262 ± 0.182	9.0 ± 4.0	—	—	—	—

Data were generated from Hill plots using pooled means (± SEM) generally from three animals for each region of brain. Cerebral cortex refers to the frontoparietal somatosensory cortex.

cortical areas display an intermediate affinity and the sites of lowest affinity are within the hippocampus and striatum. The pattern is opposite to that found for pirenzepine, thus lending further support to the suggestion that high-affinity agonist sites correspond to gallamine-sensitive M_2 sites.

In the light of recent advances in the isolation and sequencing of the muscarinic receptors derived from porcine forebrain (M_1) and atria (M_2) [25–27] and from rat brain [28], the binding of muscarinic agonists to brainstem and thalamic regions suggests that muscarinic agonists display a higher affinity for M_2 receptors than for M_1 receptors. The mRNA for M_2 receptors is found predominantly within cardiac tissue and in the brainstem and thalamus within the central nervous system [26], whereas the mRNA for M_1 receptors is found in cortical regions, especially the hippocampus [25, 28]. M_2 receptors may have an inherently higher affinity for all muscarinic agonists than M_1 receptors.

A distinction between multiple agonist sites and the existence of M_1 and M_2 receptors should be noted. The preferential binding of muscarinic agonists to M_2 muscarinic receptors does not preclude the possibility of high- and low-affinity agonist binding sites on a single receptor subtype as has been found in the cerebral cortex [18]. The binding of bethanechol and arecoline to multiple sites within the brainstem supports this possibility, although it is conceivable that multiple agonist affinities within the single brain regions may reflect small subpopulations of M_1 receptors in the midst of predominantly M_2 receptors.

The choice of selective ligands was based on criteria derived from studies on second messenger systems and from binding assays in low ionic strength buffers and guanine nucleotides. Pilocarpine has been termed an M_1-selective agonist based on the guanine nucleotide sensitivity of binding to cortical muscarinic receptors [17]; yet under the conditions utilized in the experiments outlined above, the regional selectivity was similar to that of other muscarinic agonists. It is interesting to note, however, that the relative potency of pilocarpine for hippocampal regions as compared to the thalamic regions is much higher than for the other agonists, indicating a relative selectivity for sites which are predominantly pirenzepine-sensitive (M_1) sites [5].

The presence of multiple binding sites for selective muscarinic agonists within some brain regions may reflect the ability of the ligands to interact with second messenger systems. Evidence has been presented in support of M_1 receptors linked to phosphoinositide breakdown and M_2 receptors coupled to the inhibition of adenylate cyclase based on the potency of pirenzepine inhibition [29]. Areas containing predominantly high-affinity pirenzepine (M_1) sites including the hippocampus, striatum and cerebral cortex are regions with high levels of muscarinic receptor-stimulated phosphoinositide breakdown [17]. Recent evidence indicates that M_2 receptors can couple to both adenylate cyclase and phosphoinositide turnover [30].

Bethanechol and arecoline bound to more than one site within the cerebral cortex and the paraventricular thalamus, perhaps reflecting the abilities of the agonists to recognize receptor interactions with guanine nucleotide binding proteins. Oxotremorine and pilocarpine distinguished a single site in the same regions and may not detect the coupling of receptors with different G-proteins. The capacity to bind to multiple receptors also may depend on the abilities of agonists to differentiate between receptors coupled to more than one G-protein.

It should be noted that potency in terms of binding does not always predict the most potent or efficacious ligand for second messenger systems. Oxotremorine was several orders of magnitude higher in affinity for muscarinic receptors than bethanechol in regional inhibition studies (see Table 2), yet is less effective than bethanechol in stimulating phosphoinositide breakdown in brain [17].

An additional distinction between the selectivity for second messenger systems and binding to putative muscarinic receptor subtypes concerns binding to pre- and postsynaptic receptors. Muscarinic receptors modulating acetylcholine release in the forebrain (e.g. striatum) are sensitive to gallamine [19], supporting the suggestion that at least some M_2 receptors are located on presynaptic sites [31]. Oxotremorine and pilocarpine have similar profiles of binding within the cerebral cortex and the caudate nucleus (binding to a single site, see Figs. 1 and 3), yet oxotremorine inhibits the release of acetylcholine while pilocarpine is ineffective [20, 21]. Indeed, pilocarpine behaves as a competitive antagonist in these preparations. The data presented here indicate a Hill slope near unity for pilocarpine, a property shared by most classical muscarinic antagonists.

It is possible that M_2 sites within the forebrain may possess a higher affinity for agonists, while M_1 receptors in the cerebral cortex, striatum and hippocampus located on postsynaptic terminals possess a lower affinity for muscarinic agonists. Oxotremorine activation of a single high-affinity site coupled to receptors regulating acetylcholine release and/or the inhibition of adenylate cyclase may explain both the potency of oxotremorine in the forebrain and the low efficacy for stimulating phosphoinositide turnover. It should be noted that oxotremorine binds to a single site in the cerebral cortex, suggesting that it does not distinguish (at least in terms of binding) between M_1 receptors and M_2-like presynaptic receptors in the forebrain.

Neurophysiological recordings from pyramidal cells in guinea pig cingulate cortical slices show that acetylcholine produces both a rapid hyperpolarization and a longer latency depolarization [32]. Oxotremorine is able to induce only the hyperpolarizing response which may be dependent on stimulation of GABA interneurons. In contrast, pilocarpine produces only the depolarizing response, which is most sensitive to the M_1 antagonist pirenzepine. The depolarization may be similar to that found within the CA1 of the hippocampus which is due to a decrease in K^+ conductance [33, 34]. The relative M_1-selectivity of pilocarpine and the ability to activate M_1 responses may prove useful for exploring the role of M_1 receptors in behavior. Previous studies using pirenzepine have indicated a role for M_1 receptors in memory function in experimental animals [35], suggesting that pilocarpine (or a deriva-

tive even more selective for M_1 receptors) could be used to enhance cholinergic responses at receptors involved in memory.

In summary, the binding profiles for the muscarinic agonists oxotremorine, pilocarpine, arecoline and bethanechol were determined using quantitative autoradiographic techniques. The data indicate the utility of quantitative autoradiographic methods for screening novel ligands and examining the regional selectivity of neuroactive drugs. Differences in binding properties were noted for each agonist, although the overall selectivity for brainstem and thalamic regions was similar to that found for carbamylcholine [5]. The binding data indicate that the selectivity of partial muscarinic agonists for various second messenger systems does not depend on their differential abilities to bind to subpopulations of muscarinic receptors.

REFERENCES

1. Birdsall NJM, Burgen ASV and Hulme EC, The binding of agonists to brain muscarinic receptors. *Mol Pharmacol* **14**: 723–736, 1978.
2. Ellis J and Hoss W, Analyses of regional variations in the affinities of muscarinic agonists in the rat brain. *Brain Res* **193**: 189–198, 1980.
3. Wamsley JK, Zarbin MA, Birdsall NJM and Kuhar MJ, Muscarinic cholinergic receptors: Autoradiographic localization of high and low affinity agonist binding sites. *Brain Res* **200**: 1–12, 1980.
4. Cortes R and Palacios JM, Muscarinic cholinergic receptor subtypes in the rat brain. I. Quantitative autoradiographic studies. *Brain Res* **362**: 227–238, 1986.
5. Messer WS Jr and Hoss W, Selectivity of pirenzepine in the central nervous system: I. Direct autoradiographic comparison of the regional distribution of pirenzepine and carbamylcholine binding sites. *Brain Res* **407**: 27–36, 1987.
6. Hammer R and Giachetti A, Muscarinic receptor subtypes: M1 and M2 biochemical and functional characterization. *Life Sci* **31**: 2991–2998, 1982.
7. Hammer R, Berrie CP, Birdsall MJM, Burgen ASV and Hulme EC, Pirenzepine distinguishes between different classes of muscarinic receptors. *Nature* **283**: 90–92, 1980.
8. Ellis J and Hoss W, Competitive interaction of gallamine with multiple muscarinic receptors. *Biochem Pharmacol* **31**: 873–876, 1982.
9. Stockton JM, Birdsall NJM, Burgen ASV and Hulme EC, Modification of the binding properties of muscarinic receptors by gallamine. *Mol Pharmacol* **23**: 551–557, 1983.
10. Burke RE, Gallamine binding to muscarinic M_1 and M_2 receptors, studied by inhibition of [^{3}H]pirenzepine and [^{3}H]quinuclidinylbenzilate binding to rat brain membranes. *Mol Pharmacol* **30**: 58–68, 1986.
11. Hammer R, Giraldo E, Schiavi GB, Monferini E and Ladinsky H, Binding profile of a novel cardioselective muscarine receptor antagonist, AF-DX 116, to membranes of peripheral tissues and brain in the rat. *Life Sci* **38**: 1653–1662, 1986.
12. Wamsley JK, Gehlert DR, Roeske WR and Yamamura HI, Muscarinic antagonist binding site heterogeneity as evidenced by autoradiography after direct labeling with [^{3}H]-QNB and [^{3}H]-pirenzepine. *Life Sci* **34**: 1395–1402, 1984.
13. Price M, Messer WS Jr and Hoss W, Regional distribution of muscarinic receptors preferring gallamine in the rat brain. *Biochem Pharmacol* **35**: 4171–4176, 1986.
14. Mash DC and Potter LT, Autoradiographic localization of M1 and M2 muscarine receptors in the rat brain. *Neuroscience* **19**: 551–564, 1986.
15. Olianas MC, Onali P, Neff NH and Costa E, Adenylate cyclase activity of synaptic membranes from rat striatum: Inhibition by muscarinic receptor agonists. *Mol Pharmacol* **23**: 393–398, 1983.
16. Fisher SK and Bartus RT, Regional differences in the coupling of muscarinic receptors to inositol phospholipid hydrolysis in guinea pig brain. *Neurochemistry* **45**: 1085–1095, 1985.
17. Fisher SK, Klinger PD and Agranoff BW, Muscarinic agonist binding and phospholipid turnover in brain. *J Biol Chem* **258**: 7358–7363, 1983.
18. Watson M, Yamamura HI and Roeske WR, [^{3}H]Pirenzepine and (−)-[^{3}H]quinuclidinyl benzilate binding to rat cerebral cortical and cardiac muscarinic cholinergic sites. I. Characterization and regulation of agonist binding to putative muscarinic subtypes. *J Pharmacol Exp Ther* **237**: 411–418, 1986.
19. Schoffelmeer ANM, van Vliet BJ, Wardeh G and Mulder AH, Muscarinic receptor-mediated modulation of [^{3}H]dopamine and [^{14}C]acetylcholine release from rat neostriatal slices: Selective antagonism by gallamine but not pirenzepine. *Eur J Pharmacol* **128**: 291–294, 1986.
20. Meyer EM and Otero DH, Pharmacological and ionic characterizations of the muscarinic receptors modulating [^{3}H]acetylcholine release from rat cortical synaptosomes. *J Neurosci* **5**: 1202–1207, 1985.
21. James MK and Cebeddu LX, Pharmacologic characterization and functional role of muscarinic autoreceptors in the rabbit striatum. *J Pharmacol Exp Ther* **240**: 203–215, 1987.
22. Unnerstall JR, Niehoff DL, Kuhar MJ and Palacios JM, Quantitative receptor autoradiography using [^{3}H]Ultrofilm: Application to multiple benzodiazepine receptors. *J Neurosci Methods* **6**: 59–73, 1982.
23. Paxinos G and Watson C, *The Rat Brain in Stereotaxic Coordinates*. Academic Press, New York, 1982.
24. Nonaka R and Moroji T, Quantitative autoradiography of muscarinic receptors in the rat brain. *Brain Res* **296**: 295–303, 1984.
25. Kubo T, Maeda A, Sugimoto K, Akiba I, Mikami A, Takahashi H, Haga T, Haga K, Ichiyama A, Kangawa K, Matsuo H, Hirose T and Numa S, Primary structure of porcine cardiac muscarinic acetylcholine receptor deduced from the cDNA sequence. *FEBS Lett* **209**: 367–372, 1986.
26. Kubo T, Fukuda K, Mikami A, Maeda A, Takahashi H, Mishina M, Haga T, Haga K, Ichiyama A, Kangawa K, Kojima M, Matsuo H, Hirose T and Numa S, Cloning, sequencing and expression of complementary DNA encoding the muscarinic acetylcholine receptor. *Nature* **323**: 411–416, 1986.
27. Peralta EG, Winslow JW, Peterson GL, Smith DH, Ashkenazi A, Ramachandran J, Schimerlik MI and Capon DJ, Primary structure and biochemical properties of an M_2 muscarinic receptor. *Science* **236**: 600–605, 1987.
28. Bonner TI, Buckley NJ, Young AC and Brann MR, Identification of a family of muscarinic acetylcholine receptor genes. *Science* **237**: 527–532, 1987.
29. Gil DW and Wolfe BB, Pirenzepine distinguishes between muscarinic receptor-mediated phosphoinositide breakdown and inhibition of adenylate cyclase. *J Pharmacol Exp Ther* **232**: 608–616, 1985.
30. Ashkenazi A, Winslow JW, Peralta EG, Peterson GL, Schimerlik MI, Capon DJ and Ramachandran J, An M2 muscarinic receptor subtype coupled to both adenylyl cyclase and phosphoinositide turnover. *Science* **238**: 672–675, 1987.
31. Mash DC, Flynn DD and Potter LT, Loss of M_2 muscarinic receptors in the cerebral cortex in Alzheimer's

disease and experimental cholinergic denervation. *Science* **228**: 1115–1117, 1985.
32. McCormick DA and Prince DA, Two types of muscarinic responses to acetylcholine in mammalian cortical neurons. *Proc Natl Acad Sci USA* **82**: 6344–6348, 1985.
33. Benardo LS and Prince DA, Cholinergic excitation of mammalian hippocampal pyramidal cells. *Brain Res* **249**: 315–321, 1982.
34. Benardo LS and Prince DA, Ionic mechanisms of cholinergic excitation in mammalian hippocampal pyramidal cells. *Brain Res* **249**: 333–344, 1982.
35. Messer WS Jr, Thomas GJ and Hoss W, Selectivity of pirenzepine in the central nervous system: II. Differential effects of pirenzepine and scopolamine on performance of a representational memory task. *Brain Res* **407**: 37–45, 1987.